

Fig. 70: Acid urea gel electrophoresis pattern of sperm basic nuclear proteins from fertile and study groups.

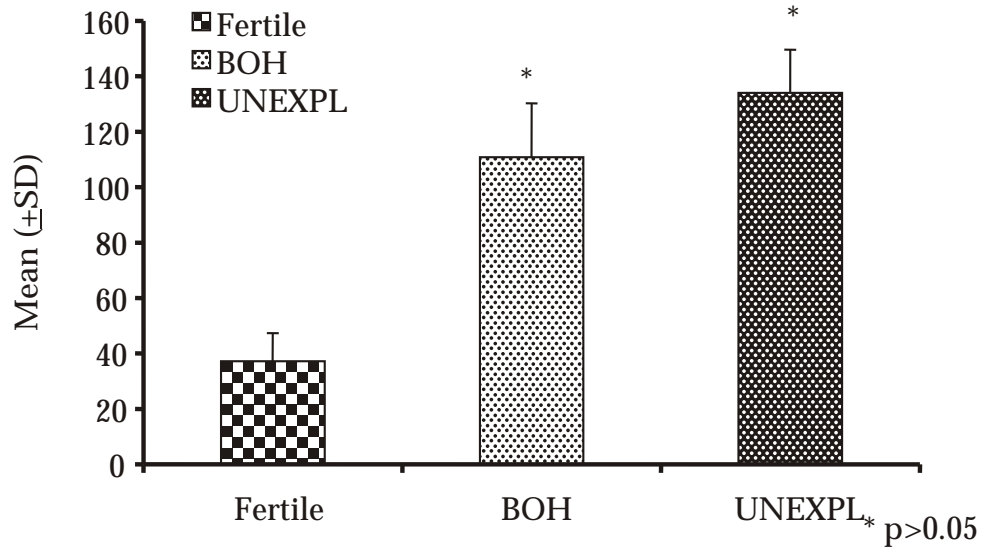


Fig. 71: A histogram depicting IOD (Mean +SD) of histones in fertile and study groups.



were observed in study groups as compared to fertile group (Figs. 74 and 75). Majority of sperm heads from the study group depicted varied abnormalities viz. dispersed chromatin, vacuolation, loss of chromatin, binucleation, loss of acrosome as well as plasma membrane etc.

An overall decrease in protamination in study groups as compared to fertile

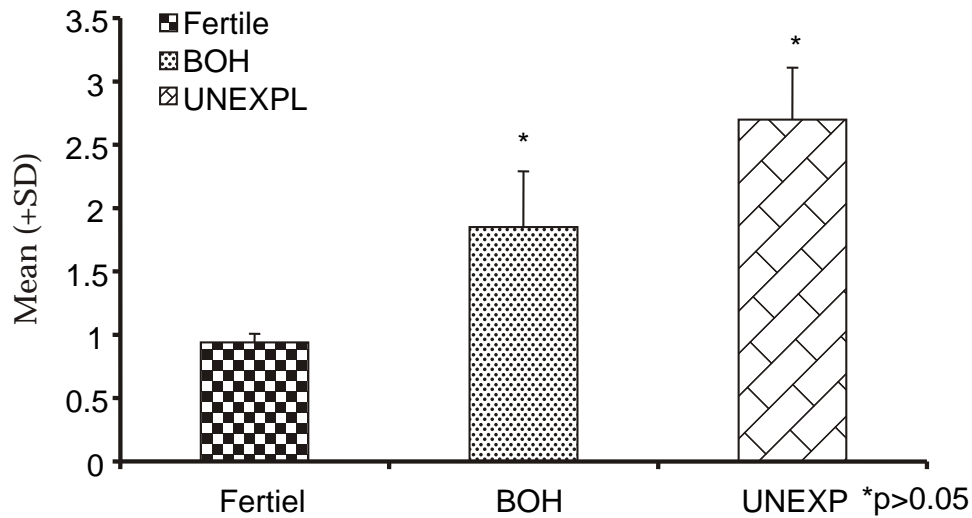


Fig. 72: (A): Western blot analysis of sperm basic proteins using monoclonal antibody against protamine 1 and protamine 2 in fertile and study groups; (B): P1/P2 ratio (IOD-Mean +SD) in control and study groups.

suggested that, proper protamination is essential for normal sperm chromatin Integrity. Altered state of sperm nuclear chromatin integrity could be the cause of BOH and unexplained male infertility.

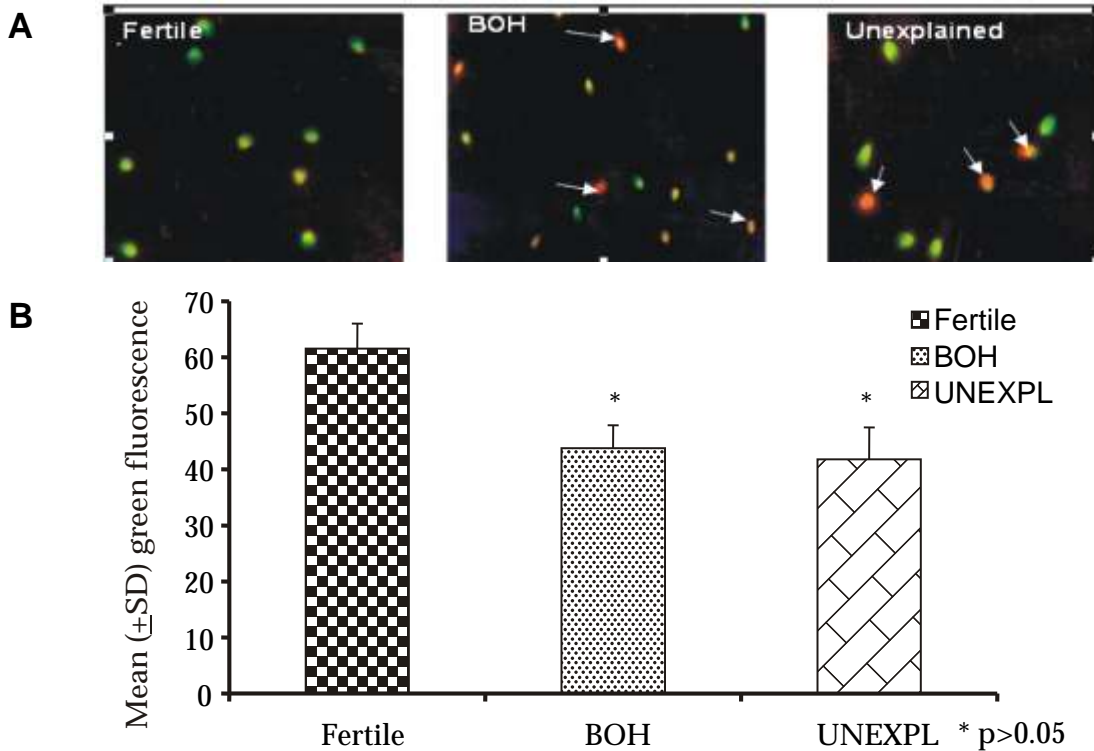


Fig. 73: (A): Acridine orange (AO) staining in control and study groups; (B): Percent AO (Mean + SD) present in control and study groups

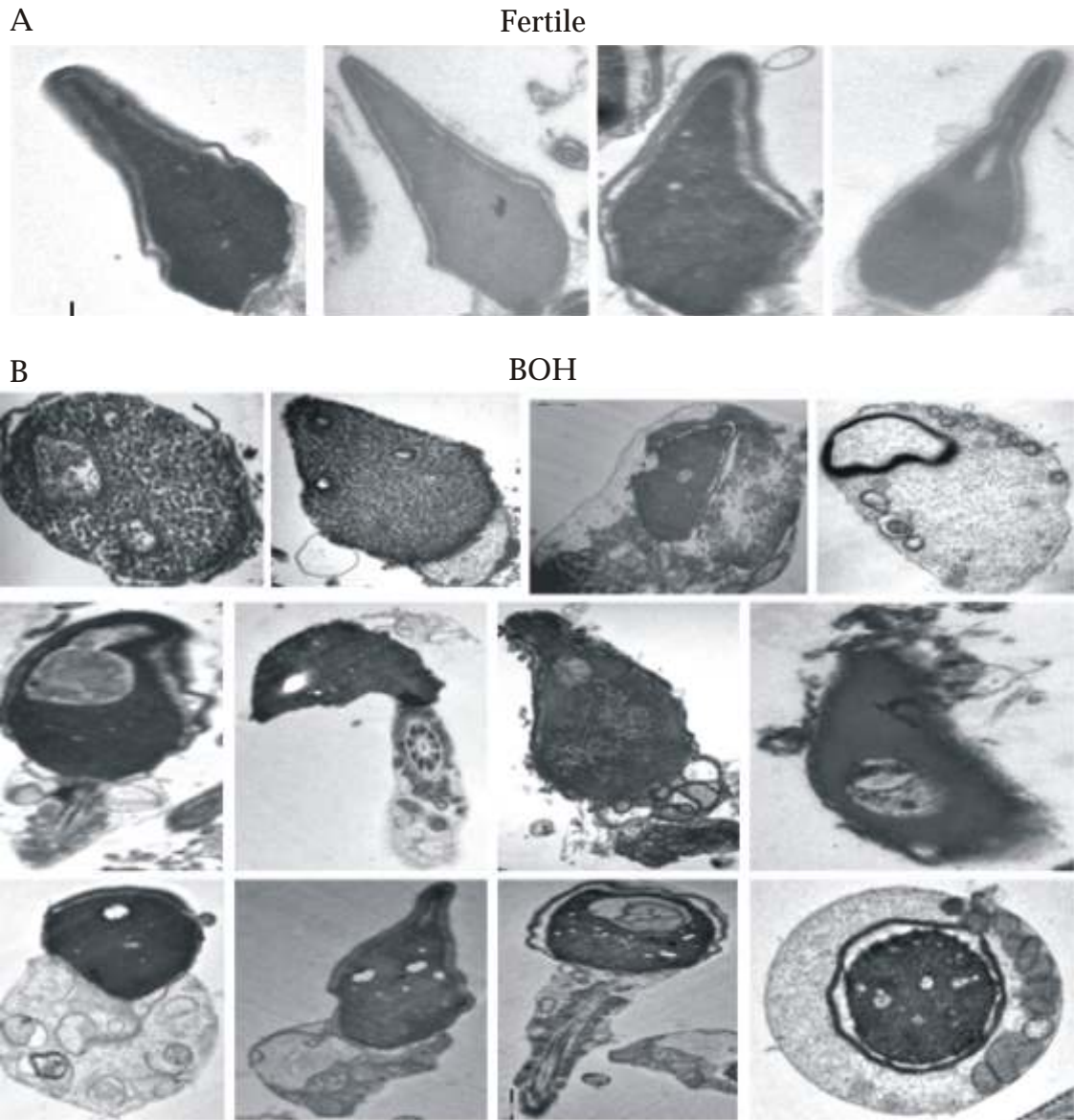


Fig. 74: Ultrastructure of sperm in fertile and BOH group.

Unexplained infertility

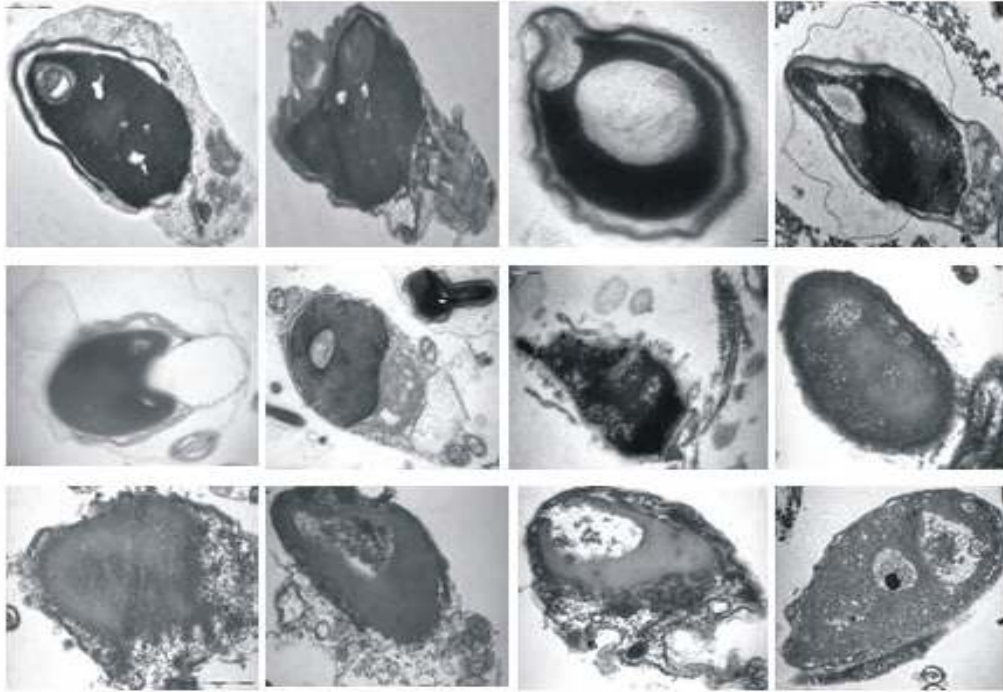


Fig. 75: Ultrastructure of sperm in unexplained group.

2.14 Studies on the Molecular Characterization of Human Sperm Progesterone Receptor

Principal Investigator: Deepak Modi

Project Associates: C.P. Puri, Geetanjali Sachdeva,
Serena D`Souza, Sushama Gadkar-Sable,
C. Shah

Duration: 1998-2007

Spermatozoa in the female reproductive tract undergo a series of biochemical modifications and exocytosis collectively termed as capacitation and acrosome reaction respectively. Both these events are indispensable for fertilization. One of the physiological initiators of acrosome reaction is the female steroid hormone progesterone. However, the receptors by which progesterone mediates these actions in spermatozoa are unknown. The aim of our studies is to identify and characterize the membrane receptor for progesterone in human spermatozoa and understand its modes of action.

Our previous studies have shown that membrane bound sperm protein binds to progesterone, but not to antiprogestins. These receptors are masked molecules that can be unmasked at capacitation or by detergent treatment. Studies were continued to

characterize this protein at molecular and functional level.

It was earlier reported that antibodies against the nuclear progesterone receptor (PR) identify a 55kDa protein in sperm lysates that has acrosomal localization and blocks progesterone binding. Using the strategy of immunopurification and proteomics approach we could successfully sequence the cognate protein identified by the nuclear PR antibodies in sperm lysates. *In silico* analysis revealed that the protein (~55kDa) identified by antibodies against the nuclear PR had homology to protein disulphide isomerase (PDI). Studies were conducted to determine if PDI is a membrane progesterone receptor.

Initial experiments were carried to determine the size, pI and localization of PDI in human spermatozoa. Using monoclonal antibody against human PDI a spot of ~55kDa with a pI of 4.6-5.2 was detected in immunoblots of sperm lysates (Fig. 76). This size and pI are identical to those reported for human PDI from somatic tissues. Immunofluorescence studies carried out on swim up preparations of human spermatozoa treated with a detergent revealed an intense localization of PDI in the acrosomal region (Fig. 77). To determine if PDI is a progesterone binding protein, immunopurified PDI was tested on ligand blots for its ability to bind labeled progesterone. Results revealed that, immunopurified PDI could bind labeled progesterone and this binding could be displaced by competition with molar excess of unlabelled progesterone (Fig. 78). Supporting these observations, antibody against PDI also blocked binding of FITC labeled progesterone on digitonin treated human spermatozoa as evident by flow cytometric quantitation. These experiments are convincing evidences to equate PDI as a candidate membrane progesterone receptor in spermatozoa. Studies are currently underway to obtain recombinant PDI and characterize the molecule for steroid specificity and binding kinetics.

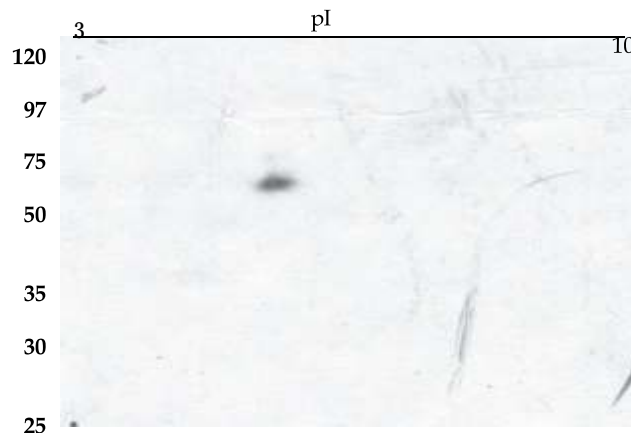


Fig. 76: Two dimensional immunoblotting for PDI on human sperm lysates separated on pI strips (3-10 non linear) and fractionated on 10% SDS PAGE.

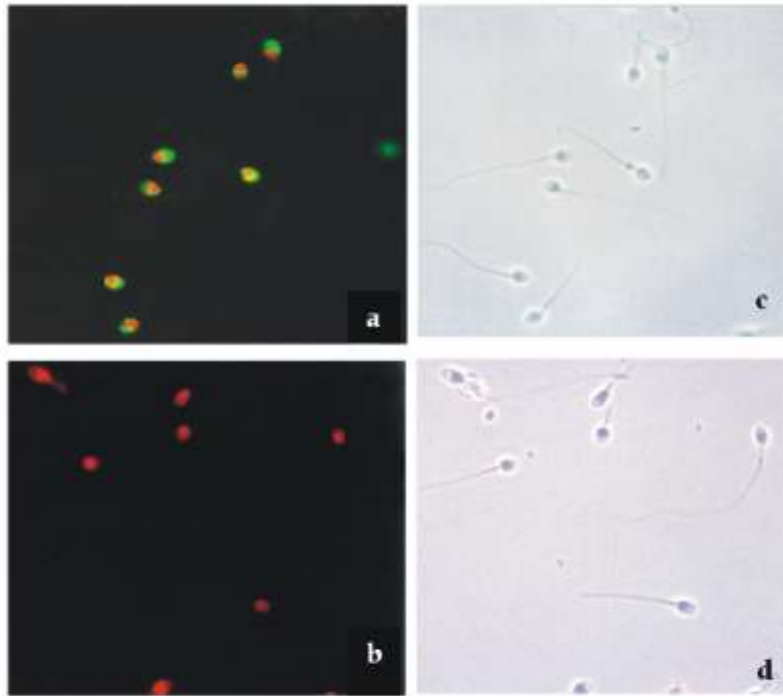


Fig. 77: Immunofluorescent localization of PDI on digitonin treated human spermatozoa. Note the green fluorescence on the acrosomal region indicating positive staining (a). The nuclei (red) are counterstained with propidium iodide. The negative control is shown in b and the respective phase contrast images are shown in c and d.

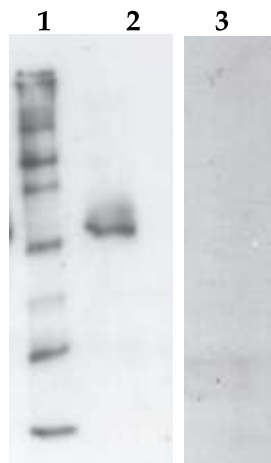


Fig. 78: Ligand blot assay of immunopurified PDI from human sperm lysates. Lane 1 labelled molecular weight markers, Lane 2 Immunopurified PDI probed with peroxidase labelled progesterone, Lane 3 immunopurified PDI probed with peroxidase labelled progesterone in presence of molar excess of cold progesterone.

2.15 Generation of Transgenic Mouse Model of Male Infertility to Study the Molecular Mechanism of Block of Spermatogenesis (*Funded by Indo-US Program*)

Principal Investigator: K.V.R. Reddy

Project Associate: M.R. Babu

Duration: 2004-2008

In humans, the azoospermic factor (AZF) on the Yq11 region is known to be involved in spermatogenesis. However, Y chromosome alone is insufficient for the regulation of spermatogenesis, since several genes are known to mediate this process. Protooncogene, c-kit receptor is one such gene with pleiotropic attributes, implicated in modulating spermatogenesis. A high level of organizational similarities exist in the localization and expression of c-kit protein in human and mouse. This suggests that the gene undergoes similar if not identical, molecular events in both species. Thus, experimental data obtained from mouse may allow direct comparison of the role played by c-kit in the human system. With this background, studies were undertaken to assess the involvement of c-kit in spermatogenesis at molecular level using transgenic approach. We expect that development of transgenic infertile mice would mimic defective spermatogenesis as seen in azoospermic, oligozoospermic and oligoasthenozoospermic men.

Molecular cloning of mouse genomic c-kit sequences

In the previous year, studies were initiated to design and construct c-kit transgene with an aim to develop transgenic mice using germ cell specific promoter. PCR amplification and cloning of RSV-LTR and c-kit promoter sequences have been reported earlier (Annual Report 2004-05, p 98). The predicted targeted transgene construct is depicted in Fig. 79. During the year, attempts were made to synthesize c-kit gene sequences. Genomic DNA was isolated from the spermatogonia of 10 day old mice and the product amplified by PCR using gene specific primers [5'- TAA AAT CAT CTT CTC TCG GAG AGC TG -3' (F); 5'- CGG AGA CAG CAG CAA AGC CTG TTG G-3' (R)]. An expected size of 630 bp PCR product was obtained. The specificity of the PCR product was improved by nested PCR using gene specific primers [5'- GGA GAG CTG AAA TGA ATG GCT GTT GCT G -3'(F); 5'- CTG CTC AGG CAT CTT CGT GCA CGA GCA G -3' (R)] and the c-kit gene was amplified using first PCR product as template (Fig: 80). The PCR product obtained was sequenced and the sequence confirmed. The product was cloned in pMosblue vector at EcoRV site and transformed into *E.coli* competent cells. -gal assay system was used to screen the clones. The presence of insert was confirmed by colony PCR (Fig. 81).

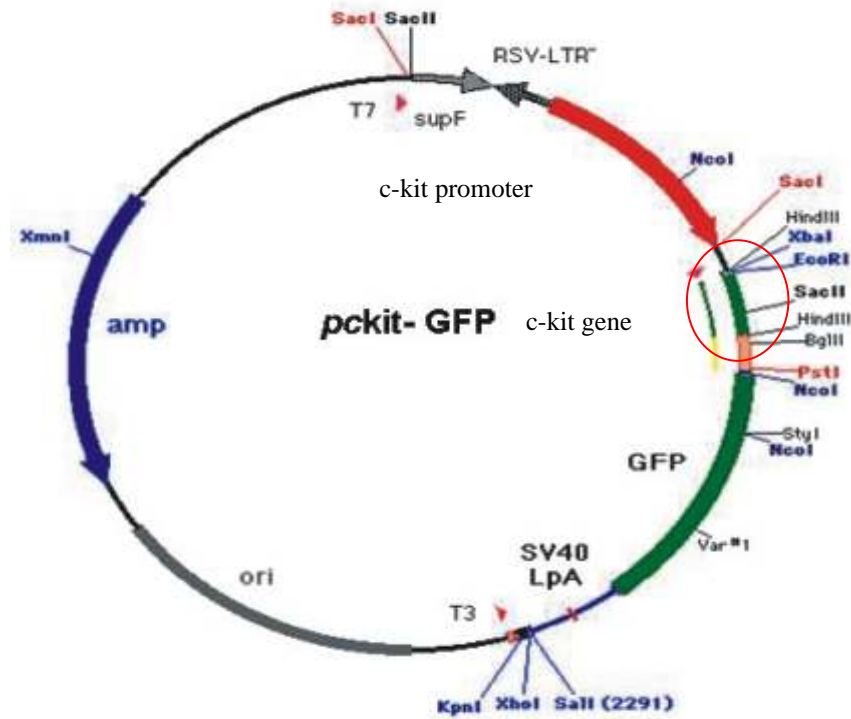
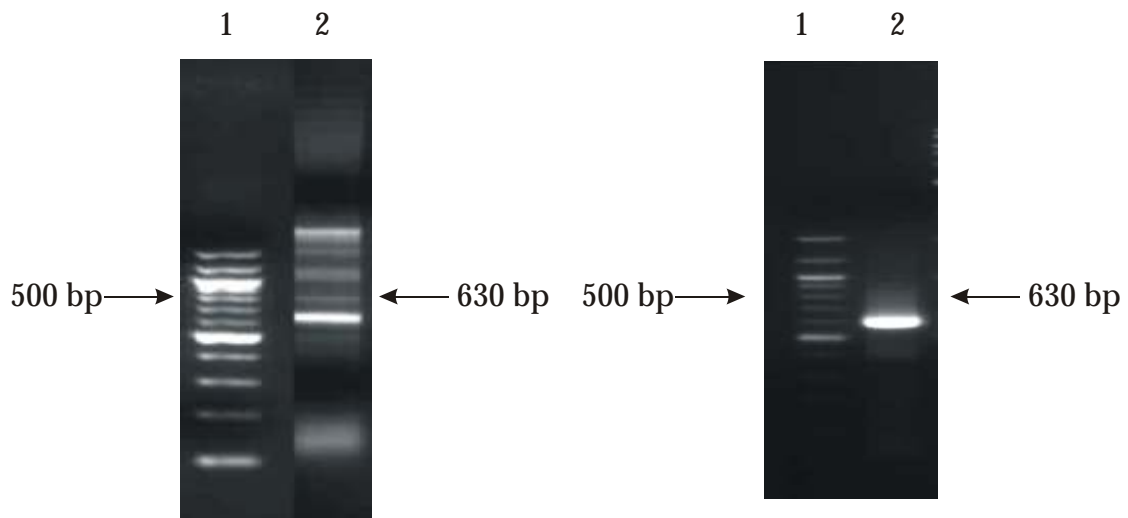


Fig. 79: Predicted model of c-kit GFP transgene construct.



1= Amplification of c-kit by primary PCR
2= 100 bp marker

1= Amplification of c-kit by nested PCR
2= 500 bp marker

Fig. 80: Amplification of c-kit gene by PCR and nested PCR.

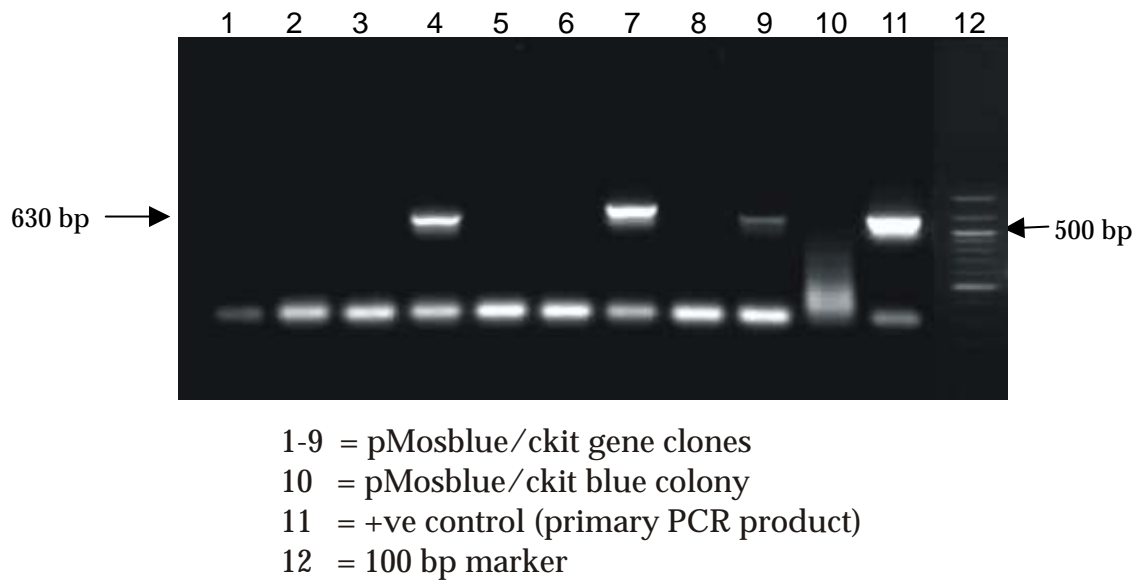


Fig. 81: Colony PCR of pMosblue/ c-kit gene clones. Clone 4 & 7 are +ve for c-kit gene insert.

2.16 Regulation of Spermatogenesis by Estrogen

2.16.1 Effect of Estrogen/Antiestrogen on Germ Cell Maturation in the Testis

Principal Investigator: Nafisa Balasinor

Project Associates: Manjit Sharma, R. D'Souza and
Niraja Paradkar

Duration: 2002-2007

A disorganization of the seminiferous epithelium cytoarchitecture was observed earlier with tamoxifen and estradiol treatment, presumably affecting germ cell maturation, ultimately leading to the observed decrease in fertility. The study suggested that Sertoli cell to germ cell interaction within the seminiferous tubule could be affected (Annual Report 2000-2001, p 95). Subsequent studies on the effect of tamoxifen treatment on cell adhesion molecules viz integrin 61, Cadherin and integrin linked kinase, known to be localized in the adherens junction and involved in cell-cell interaction demonstrated stage specific decrease in the localization of these proteins following tamoxifen treatment (Annual Report 2003-04, p 197). Since tamoxifen had decreased the intratesticular testosterone, it remained to be seen if the effect is due to reduced testosterone or due to the antiestrogenic/estrogenic effect of the drug.

In order to study the direct effect of estrogen on the seminiferous epithelium, two doses of 17- estradiol, viz 20 and 100 g/kg/day were administered subcutaneously to adult male rats for a period of 10 days and the effect on serum hormones and intratesticular testosterone (T) and estrogen (E) was studied. Estradiol at the dose of 20 µg/kg/day affected the hypothalamus pituitary axis reducing serum gonadotrophins and intratesticular testosterone, while at the dose of 100 µg/kg/day decreased serum FSH and intratesticular testosterone but increased intratesticular estradiol without affecting serum LH levels (Annual Report 2004-05, p 101).

Beside the effect on hormones, in the testis, morphologically two visible effects were seen. Spermiation Failure (Fig. 82) was seen at both the doses. This was attributed to the suppression of T and FSH. An 'Antiapoptotic Effect' observed at the dose of 100 µg/kg/day could have been due to the increase in intratesticular E. The direct effect of an increase in intratesticular estradiol levels with 100 µg/kg/day was observed in terms of a decrease in apoptosis in germ cell when compared to 20 µg/kg/day (Annual Report 2004-05, p 101). The study suggested that 20 and 100 µg/kg/day of 17- estradiol could be used to study the direct effect of high intratesticular estradiol concomitant with decreased intratesticular T and serum FSH levels on spermatogenesis.

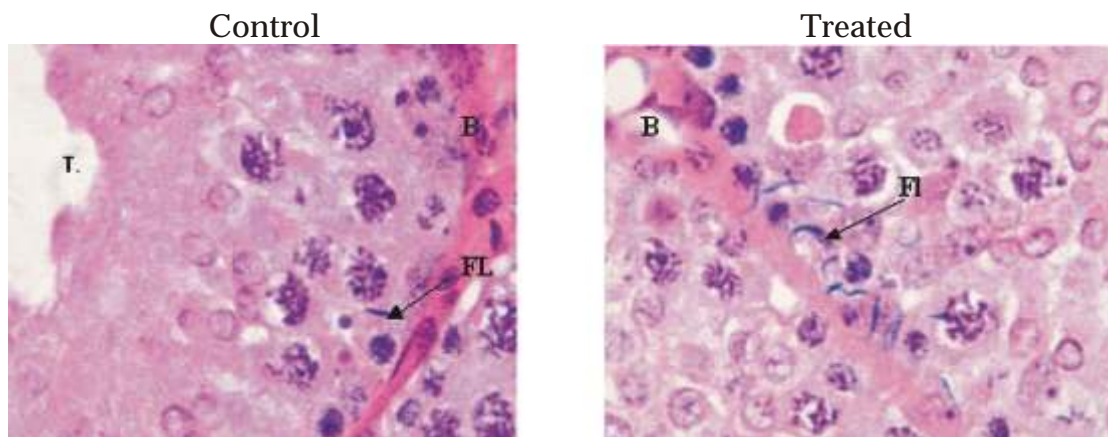


Fig. 82: Five micron sections of testis from adult male rats stained with haematoxylin and eosin showing the stage IX specific effects. Left panel represents control group Right panel represents estradiol treated group with a dose of 20 µg/kg/day for 10 days. 'Fl' indicates failed spermatids, 'L' indicates lumen, 'B' indicates basement membrane (Magnification 1250X)

In the reporting year, stage specific expression of cell adhesion molecules (Pan Cadherin and Beta Catenin) and cytoskeletal proteins (F Actin, Vimentin and Beta Tubulin) in the control and 20 µg/kg/day estradiol treated testis samples was studied. In addition, a study on the differential global gene expression profile between the two doses by microarray was initiated.

It was observed that each protein showed a cell and stage specific pattern of expression. Positive Tubulin staining was seen in the Sertoli cell originating from the base and extending towards the lumen (Fig. 83). Vimentin staining was restricted to the regions around the Sertoli cell nucleus showing a branched structure in stages I- V while a perinuclear staining during spermiation in stages VII-VIII (Fig. 84). Both P Cadherin and beta Catenin showed staining around the elongating and elongated spermatids where the ectoplasmic specialization an actin based adheren junctions are present, additionally these proteins were also localized at the level of tight junctions close to the base of seminiferous epithelium (Fig. 85). F actin was seen to be present around elongating and elongated spermatids (Fig. 86). There was a stage specific effect on the expression of both cell adhesion molecules and cytoskeletal proteins in the testis of estradiol treated animals. Stages I- VII and stages XI- XIV being unaffected and certain proteins namely Tubulin and Pan Cadherin were seen associated with the failed spermatids in stage XI of spermatogenesis (Fig. 87). The expression of these proteins associated with failed spermatids will be further studied at the ultrastructural level.

Microarrays analysis of testicular RNA from control and estradiol treated rats were done using Rat Genome U34A Array from Affymetrix, USA; containing 8799 genes. Preliminary results revealed that 128 genes were differentially expressed in the control (C) vs 20 µg/kg/day estradiol treated group (E20) and 166 genes were differentially expressed in the C vs 100 µg/kg/day estradiol treated group (E100) (Fig. 88 & 89A, B). A comparison of the E20 and E 100 revealed 88 differentially expressed genes. Further work on pathway analysis and then confirming these differentially expressed genes by RT PCR or Real time PCR will be undertaken.

2.16.2 Genomic Imprinting: A Paternal Contribution to Embryogenesis

Principal Investigator: Nafisa Balasinor

Project Associates: Manjit Sharma, Shilpa Pathak, Neelam Kedia
and Madhurima Saxena

Duration: 2002-2007

The significance of paternal genome/factor during embryogenesis is highlighted by numerous studies concluding biasness of paternal genome towards development of extra embryonic structures thereby promoting embryo growth. This non-equivalence of parental genomes is genomic imprinting and many genes are expressed in an imprinted fashion during embryonic development. Insulin-like growth factor (*Igf2*) is an imprinted gene expressed in the embryo from the paternal allele. *Igf2* signaling through its cognate receptor, *Igf1r* promotes early embryo growth and development. The paternal specific expression of *Igf2* is dependent on

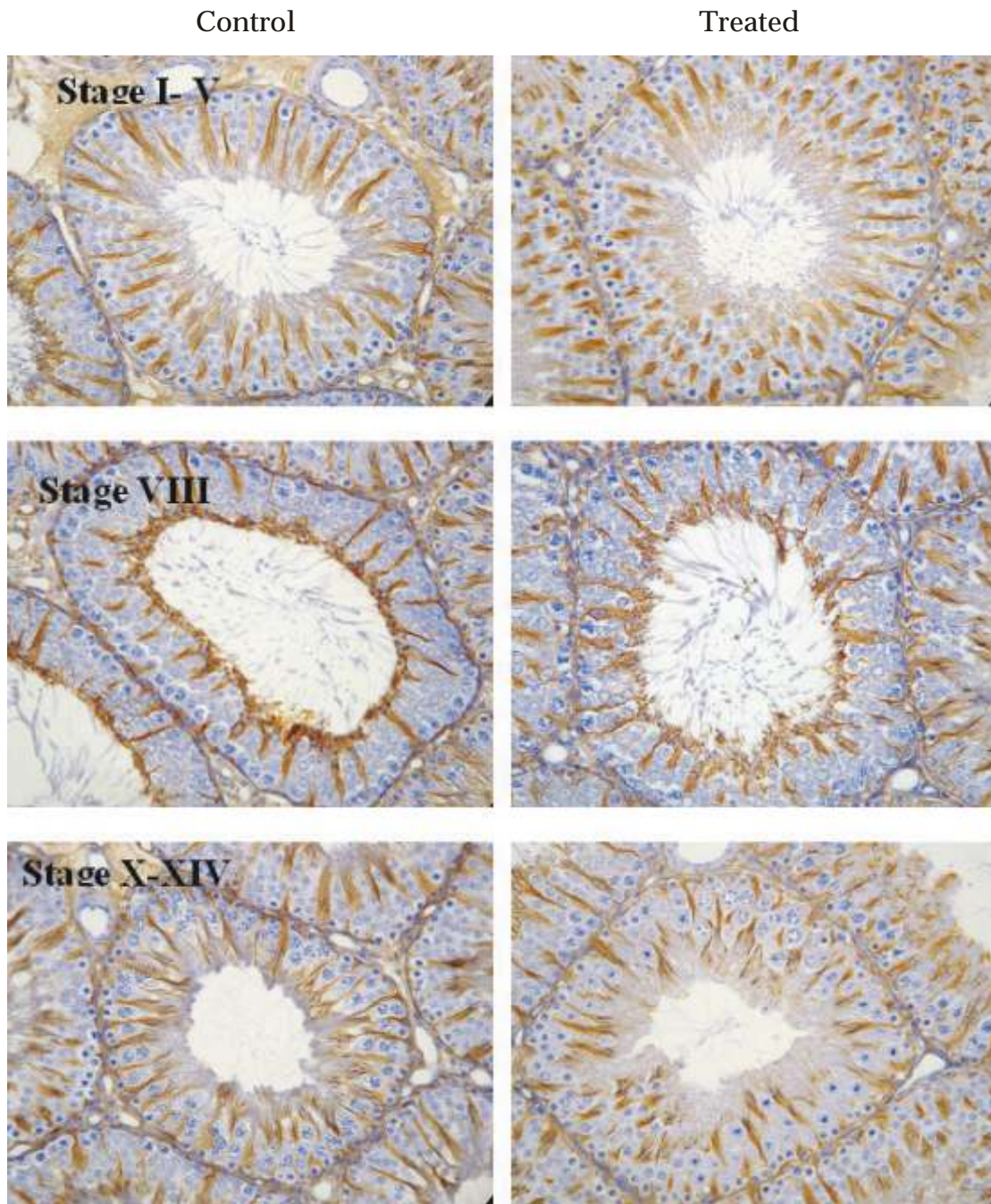


Fig. 83: Immunohistochemical localization of beta Tubulin in the seminiferous tubule showing stage specific expression. Left panel for control group and right panel for estradiol treated group with a dose of 20 $\mu\text{g}/\text{kg}/\text{day}$ for 10 days. (Magnification 450X)

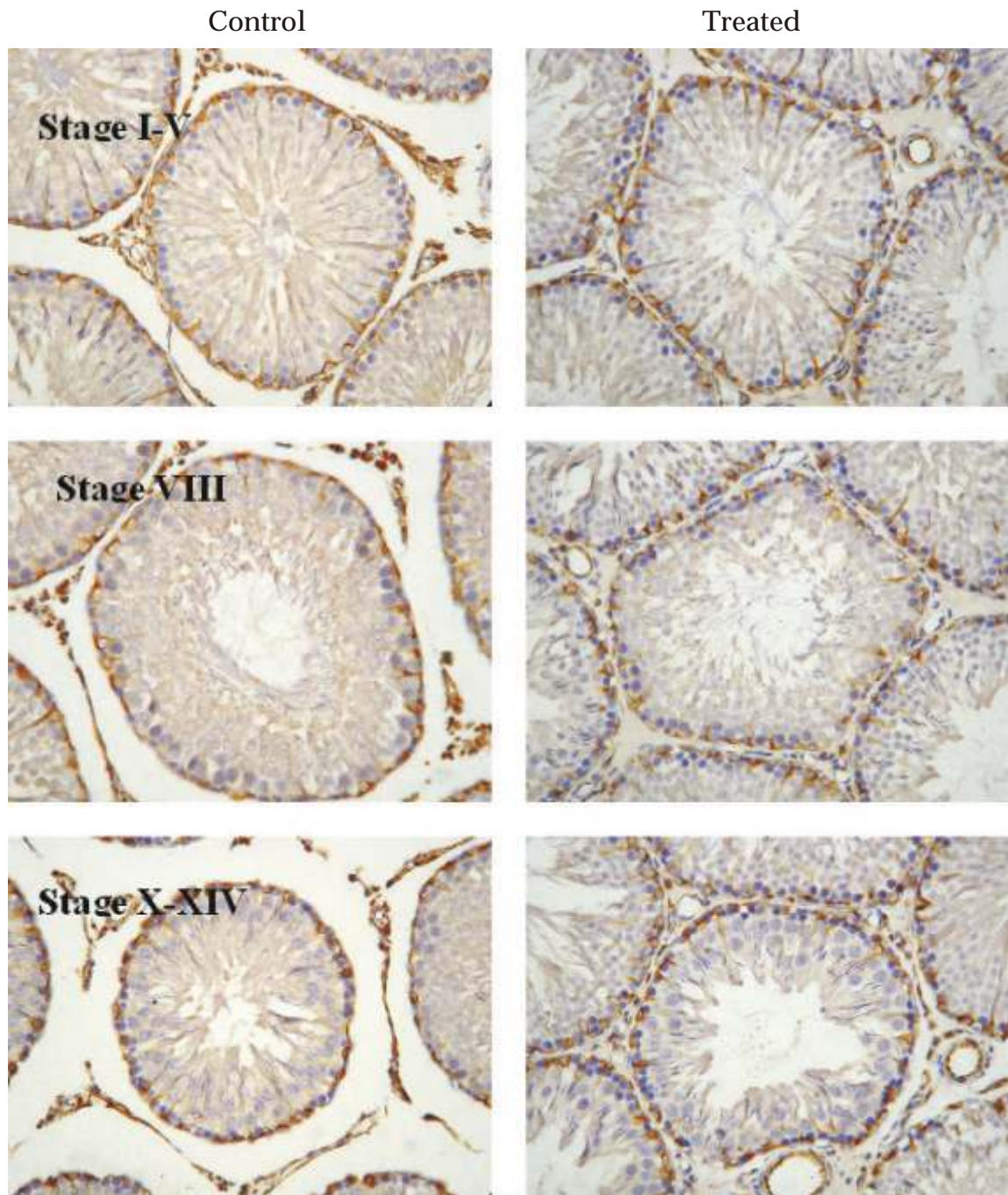


Fig. 84: Immunohistochemical localization of vimentin in the seminiferous tubule showing stage specific expression. Left panel for control group and right panel for estradiol treated group with a dose of 20 $\mu\text{g}/\text{kg}/\text{day}$ for 10 days. (Magnification 450X)

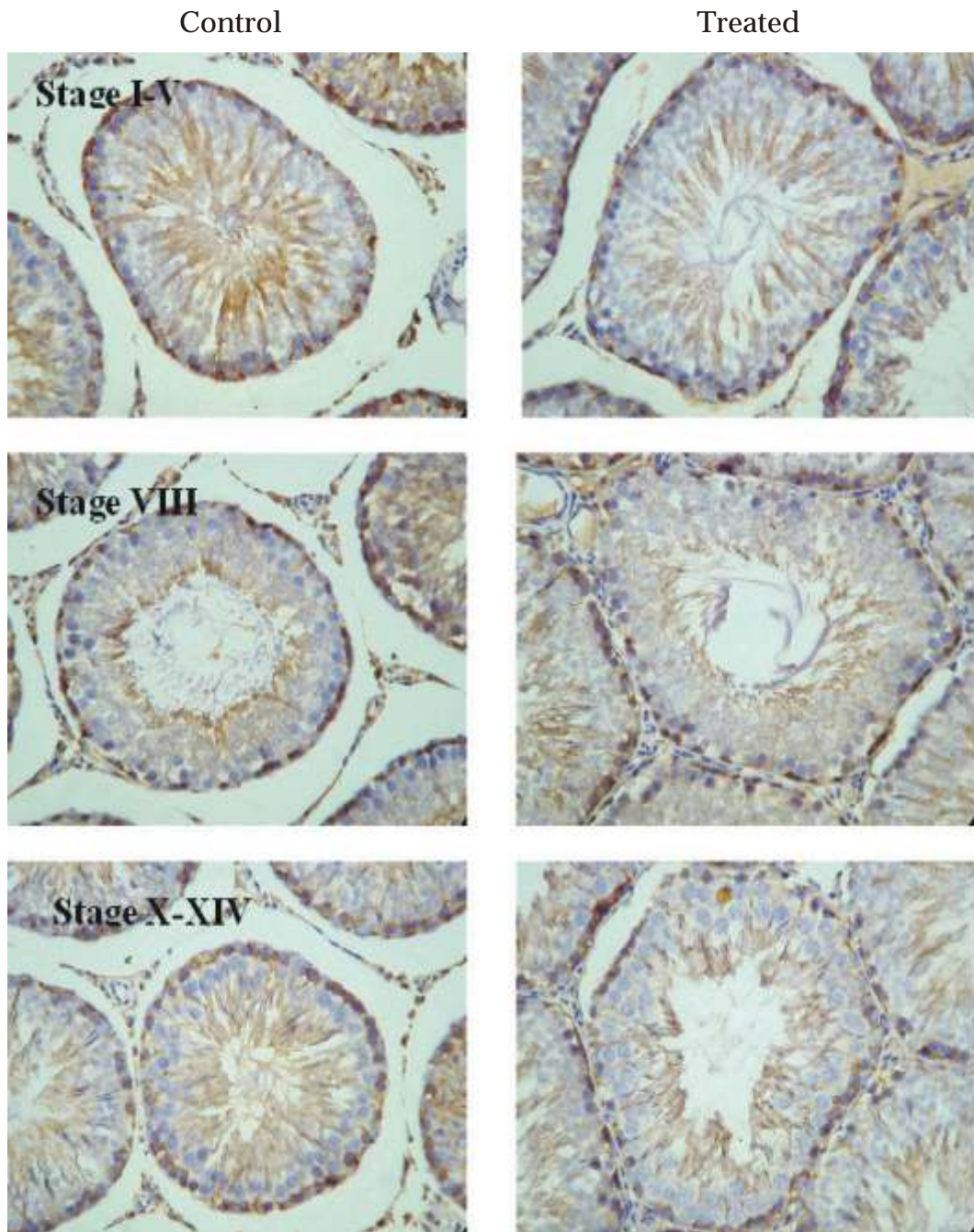


Fig. 85: Immunohistochemical localization of Pan Cadherin in the seminiferous tubule showing stage specific expression. Left panel for control group and right panel for estradiol treated group with a dose of 20 $\mu\text{g}/\text{kg}/\text{day}$ for 10 days. (Magnification 450X)

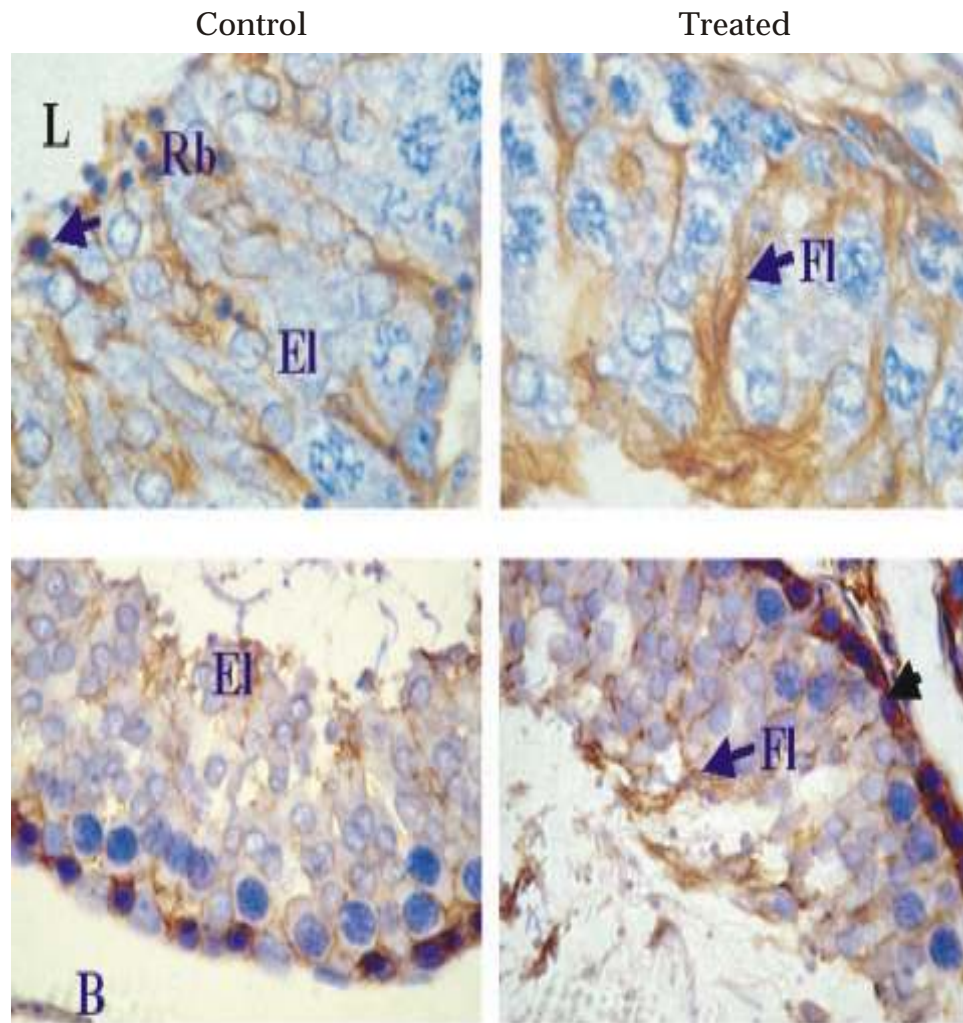


Fig. 86: Upper Panel: Immunohistochemical localization of beta Tubulin in the seminiferous tubule showing stage IX control (left) and treated (right) group with a dose of 20 $\mu\text{g}/\text{kg}/\text{day}$ for 10 days. Lower Panel: Immunohistochemical localization of Pan Cadherin in the seminiferous tubule showing stage IX control (left) and treated (right) group with a dose of 20 $\mu\text{g}/\text{kg}/\text{day}$ for 10 days. 'Fl' indicates failed spermatids, 'B' indicates basement membrane, 'Rb' indicates residual bodies, 'El' indicates elongating spermatids. Arrow indicates positive staining around the failed spermatids and small arrow in the lower panel indicate positive staining at the tight junction (Magnification 1250X)

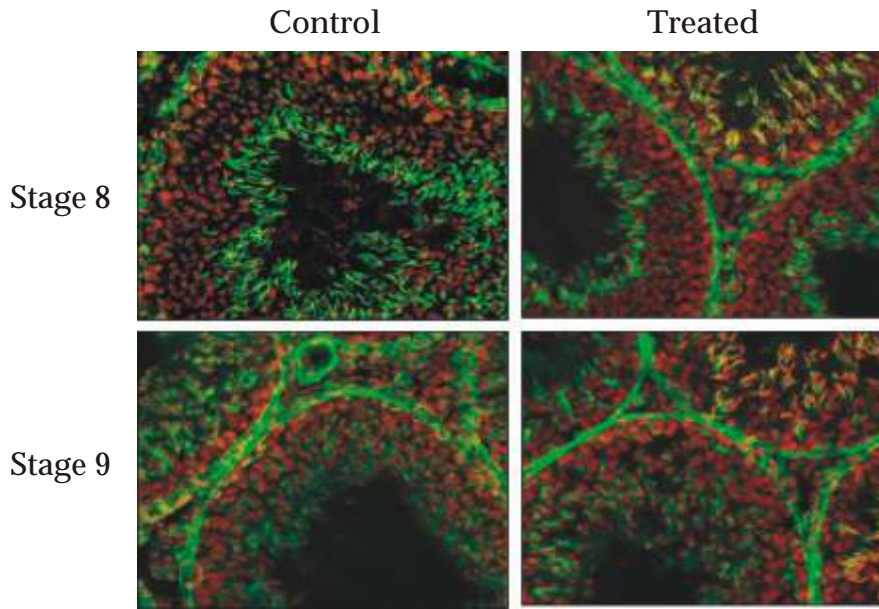


Fig. 87: Upper Panel: Localization of F actin on eight micron cryosections in the seminiferous tubule showing stage VIII of spermatogenesis in control and treated animals. Lower Panel: Localization of F actin on eight micron cryosections in the seminiferous tubule showing stage IX of spermatogenesis in control and treated animals.

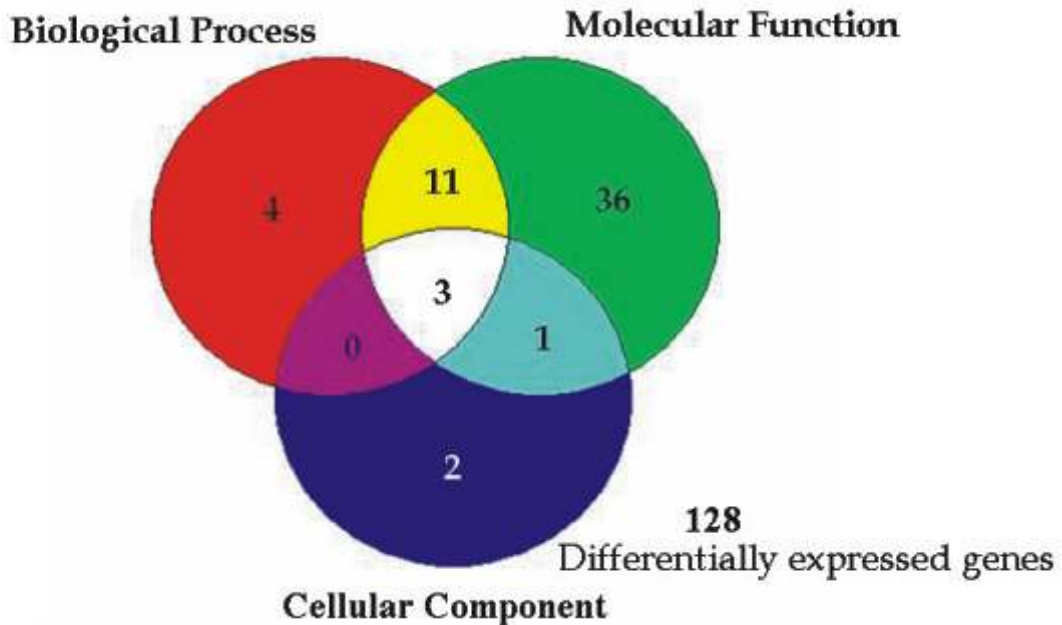


Fig. 88: Venn diagram representing differentially expressed genes by microarray in Control Vs E20 dose depicting genes involved in biological processes (Red), cellular processes (blue) and Molecular processes (green).

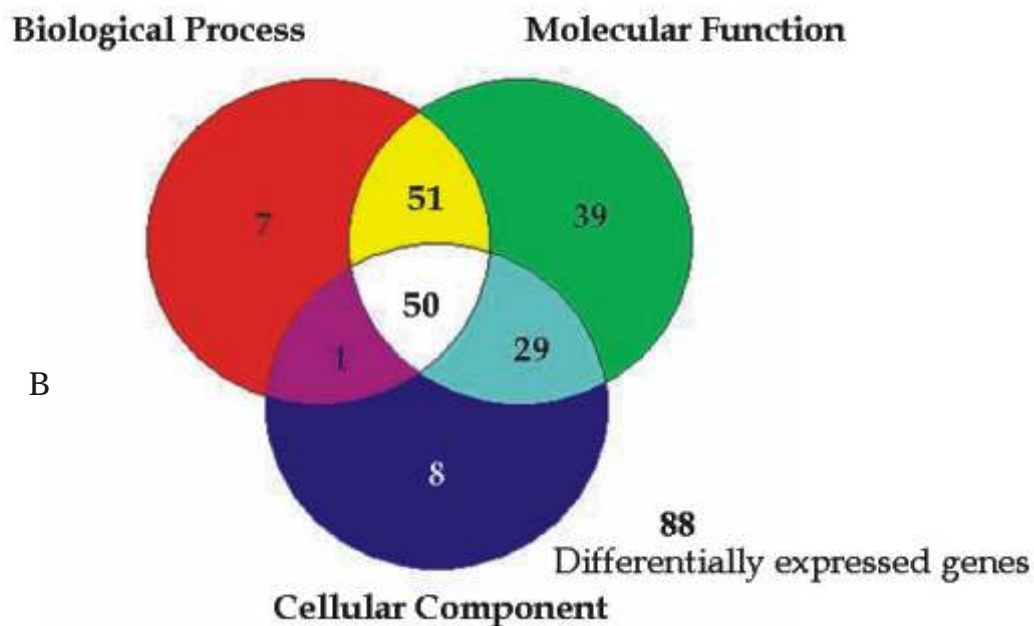
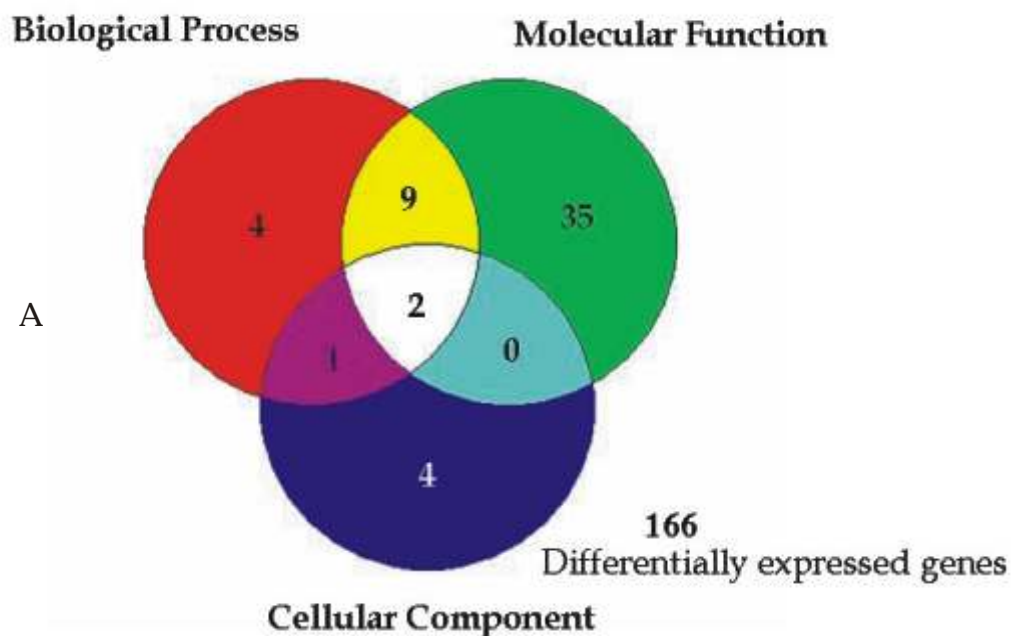
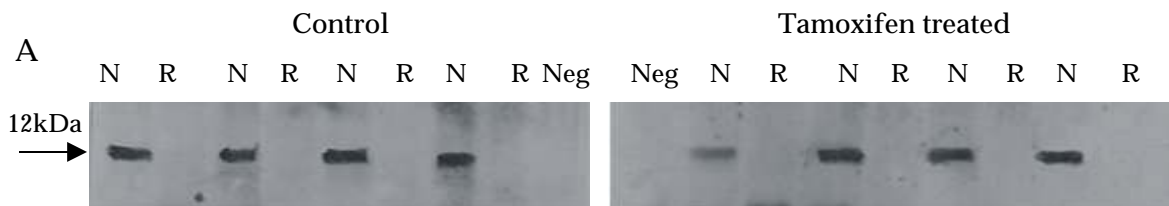


Fig. 89: (A): Venn diagram representing differentially expressed genes by microarray in Control Vs E100 dose depicting genes involved in biological processes (Red), cellular processes (blue) and Molecular processes (green). (B): Venn diagram representing differentially expressed genes by microarray comparing the two doses namely E20 Vs E100 depicting genes involved in biological processes (Red), cellular processes (blue) and Molecular processes (green).

methylation of imprinting control region (*ICR*) located downstream of *Igf2* during spermatogenesis in the male germ line. Our previous studies have demonstrated an increase in pre- and post-implantation loss following tamoxifen treatment to adult male rats at a dose 0.4 mg / kilogram body weight/ day for 60 days. The objective of the present study was to investigate a relationship between paternal epigenetic contribution in terms of DNA methylation both global as well as at *ICR* in the male germ line and its effect on the embryo development in the subsequent generation. The specific objectives were to (i) study the effect of paternal tamoxifen exposure on the localization and expression of *Igf 2* and *Igf* type 1receptor (protein and mRNA) in post-implantation embryos (ii) study the effect of tamoxifen treatment to adult male rats on the methylation pattern of paternally expressed genes (*Igf2*) in the spermatozoa and its correlation to embryo development of the subsequent generation (iii) study the effect of tamoxifen treatment to adult male rats on the global DNA methylation of the spermatozoa and its correlation to embryo development.

Igf2 mediates mitogenic response via *Igf1r* thereby modulating embryo growth around day 9-11 of gestation in rodents. The expression of *Igf2* and *Igf1r* transcript was reported earlier (Annual Report 2002-03, p 136). Expression of *Igf2* protein in normal and resorbed embryo was studied this year by western blot analysis. A specific band of ~12 kDa was detected with anti-*Igf2* antibody in the normal embryos from both control and treated group. This band was absent in the resorbed embryos from both the groups (Fig. 90).

Western blot with anti-*Igf1r* detected 2 bands, ~200 kDa representing the precursor protein and ~97 kDa band corresponding to the mature protein (Fig. 91A). A significant decrease in both the proteins was observed in the resorbed embryos from both control and treated groups (Fig. 91B and 91C). This result suggests that decrease in *Igf2* and *Igf1r* mRNA and protein could be one of the factors responsible for resorptions.



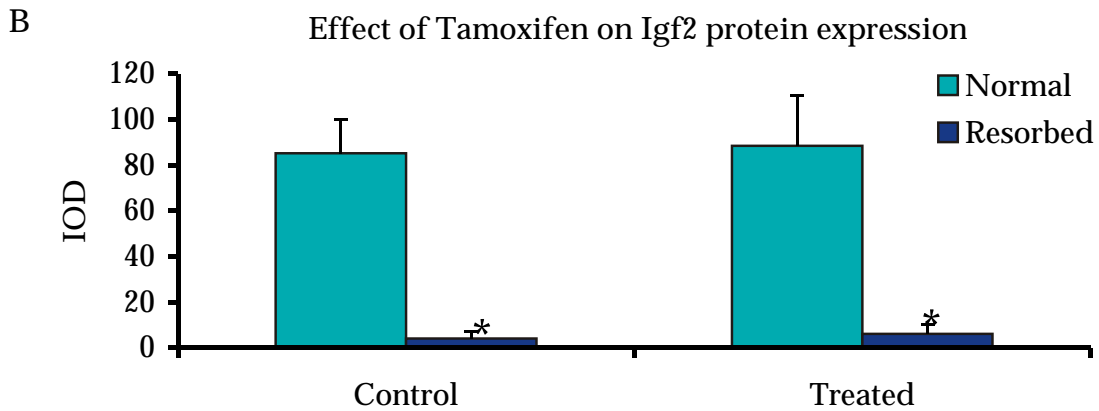
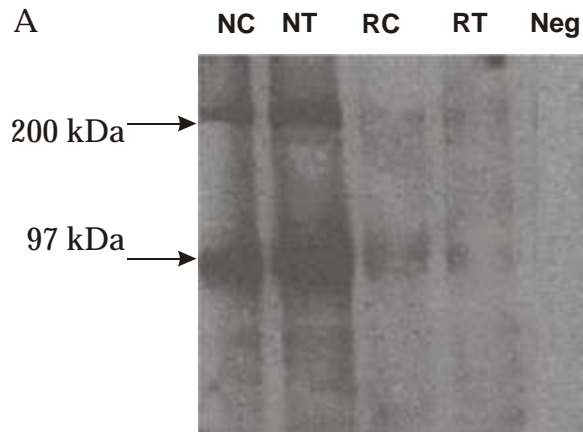


Fig. 90: (A): Representative western blot of Igf2 in 13-day-old normal (N) and resorbed (R) embryos sired by control and tamoxifen treated male rats. M represents molecular weight marker. Neg represents only secondary control. (B): Expression of Igf2 protein in 13-day-old normal (N) and resorbed (R) embryos in control and treated group. The values represent mean \pm s.d. ($n=6$ in each group). “*” denotes significance with respect to the normal embryos ($p<0.05$).

Igf2 is paternally expressed imprinted gene on rat chromosome 1 exhibiting reciprocal imprinting pattern with neighboring maternally expressed *H19* gene. These genes are coordinately regulated by *ICR* positioned between *Igf2* and *H19* and interaction of *ICR* with common enhancer elements. The coordinate regulation of expression of *Igf2* and *H19* is largely dependent on DNA methylation of *ICR*. In the spermatozoa, *DNA ICR* is methylated while the oocyte *DNA* shows nonmethylated *ICR*. *Igf2-H19 ICR* locus specific methylation was analyzed by methylation specific PCR (MS-PCR). MS-PCR analysis was performed on bisulfite-modified sperm DNA using MS-PCR primers specific for methylated (M) and unmethylated DNA (U).



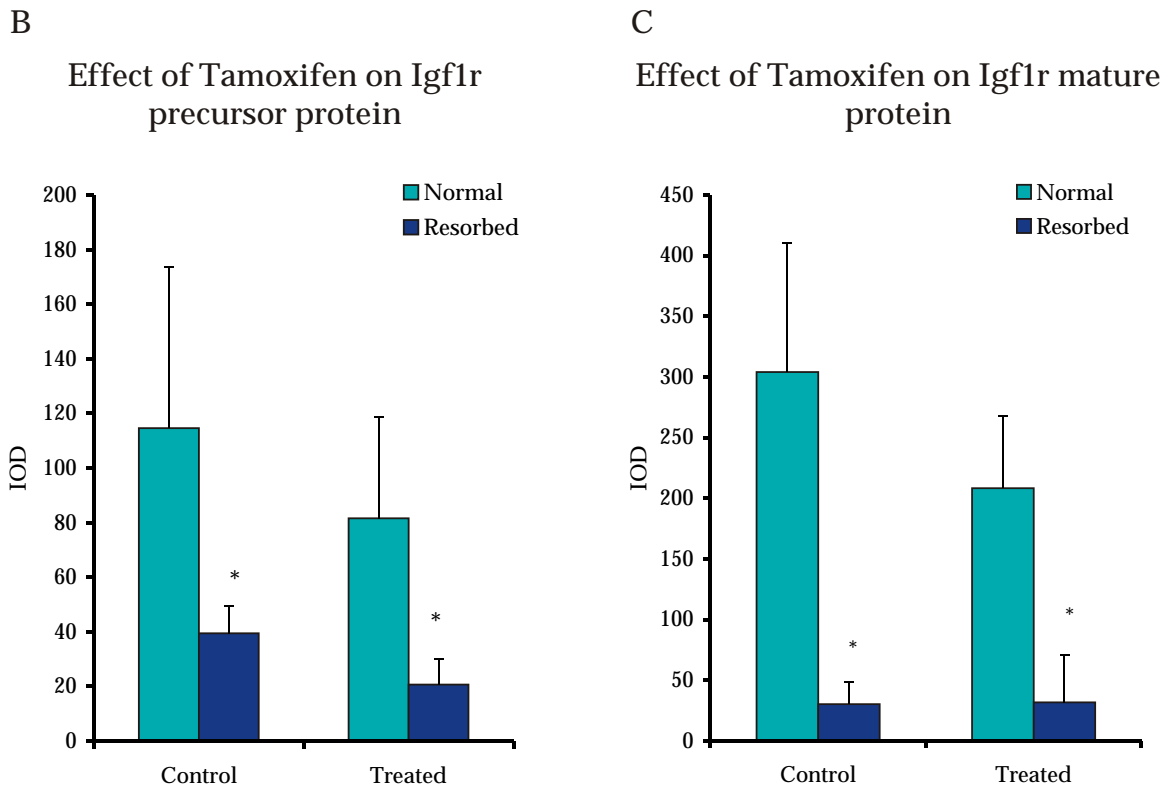


Fig. 91: (A): Representative western blot of Igf1r protein in 13-day-old normal (N) and resorbed (R) embryos by control (C) and tamoxifen treated (T) group. Lane NC: Normal fetus from control group; lane NT: Normal fetus from Treated group; Lane RC: Resorbed fetus from control group; Lane RT: Resorbed fetus from treated group. (B and C): Expression pattern of Igf1r precursor protein (200 kDa) and mature protein (97 kDa) in the normal and resorbed embryos in control and treated group. Values represent mean IOD s.d. ($n=6$ in each group). “*” denotes significance with respect to the normal embryos ($p < 0.05$).

MS-PCR on bisulfite modified sperm DNA from control and tamoxifen-treated group showed 3 different PCR patterns i.e. pattern A, B and C. Pattern A showed amplification with “M” primer but not with “U”. Pattern B revealed amplification with both, “M” and “U” primers whereas pattern C displayed amplification with “U” primers but not with “M” (Fig. 92A). Pattern A indicated methylation of CpG island at *Igf2-H19* locus whereas pattern C specified loss of methylation. Pattern B denoted heterogeneous sperm populations with methylated and unmethylated CpG island at *Igf2-H19* locus. The MS-PCR pattern correlated well with the tamoxifen treatment. Sperm samples from control male rats displayed pattern A and B correlating with resorption whereas majority of spermatozoa samples from tamoxifen treated group showed pattern B and C significantly correlating with resorption (Fig. 92B). Thus the pregnancy outcome appears to be a

consequence of tamoxifen induced loss of methylation at CpG island at *Igf2-H19* locus in the spermatozoa.

Igf2 has a tissue specific monoallelic expression in the embryo. MS-PCR on bisulfite modified liver DNA from normal fetuses from control and tamoxifen-treated groups showed amplification with both, “M” and “U” primers (Pattern B) whereas resorbed fetuses from both the groups showed pattern C displaying amplification with “U” primers but not with “M” (Fig. 93). Thus, resorbed embryos show loss of methylation indicating common mechanism of resorption in control and tamoxifen treated groups.

Global methylation was analyzed by immunostaining spermatozoa with 5-methyl cytosine antibody followed by flow cytometric analysis (Fig. 94A). The global methylation level (GML) of sperm DNA was quantitated as Mean Fluorescence Intensity. Sperm GML was not affected by tamoxifen treatment. When sperm GML was correlated to POL, in both, control and treated groups, no association was found between sperm GML (MFI) and POL (Fig. 94B and C) suggesting *Igf2-H19 ICR* locus specific effect of tamoxifen. The pregnancy outcome was found to be independent of global DNA methylation of sperm.

In conclusion, our results show a correlation between methylation at *Igf2-H19 ICR* in spermatozoa, embryo development and pregnancy outcome. This signifies *Igf2-H19 ICR* methylation in spermatozoa as a predictive factor to assess embryonic development. Secondly, the study also shows a correlation of methylation at *Igf2-H19 ICR* in spermatozoa and tamoxifen treatment indicating an effect of tamoxifen in the establishment and/or maintenance of methyl imprint during spermatogenesis.

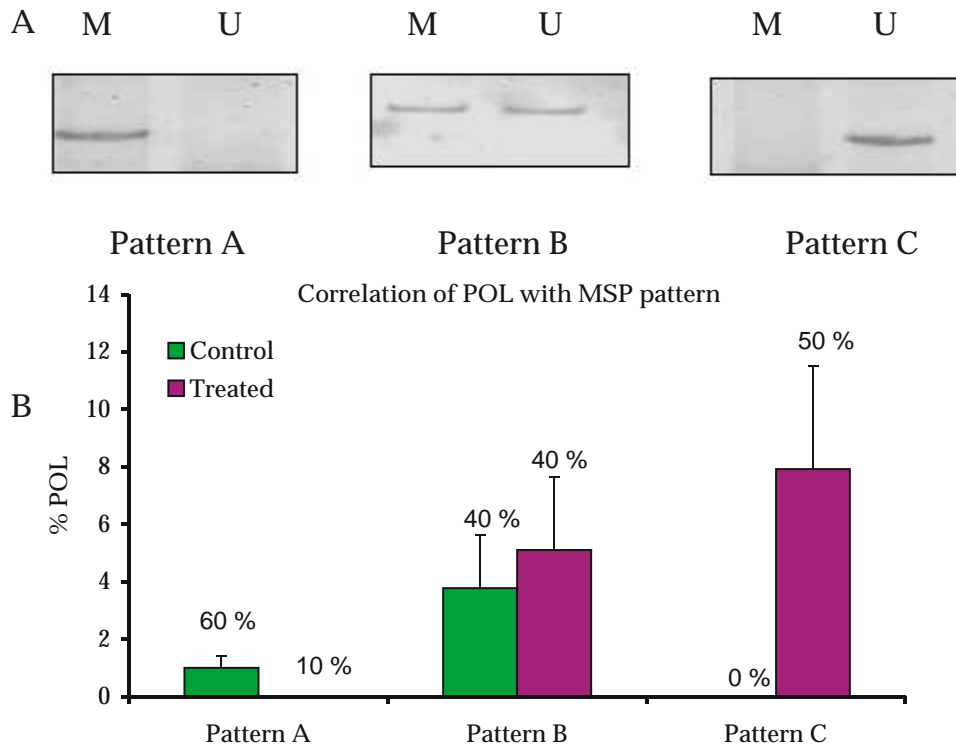


Fig. 92: (A): 3 emergent patterns from methylation specific PCR of CpG island at *Igf2-H19* locus in sperm from control and tamoxifen treated group. Pattern A: amplification with “M” primer but not with “U”; pattern B: amplification with both, “M” and “U” primers; pattern C amplification with “U” primers but not with “M”. (B): Distribution of pregnancy outcome (% POL) according to the 3 emergent MS-PCR patterns at *Igf2-H19* locus in spermatozoa in control and tamoxifen treated group. % Values indicate sample distribution in each treatment group (n=10 for each group) and bars indicate % POL represented by mean s.e.m. “*” denotes significance with respect to % POL in pattern A ($p < 0.05$).

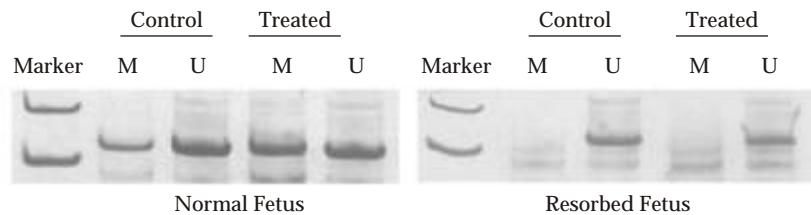


Fig. 93: Representative silver-stained 10% polyacrylamide gel after a PCR amplification of CpG island at *Igf2-H19* locus following bisulfite modification of normal and resorbed fetal DNA from control (C) and tamoxifen treated (T) group. Primers specific for methylated (M) and non-methylated (U) DNA were used.

